Anal Bioanal Chem (2015) 407:3883–3897
DOI 10.1007/s00216-014-8411-6

REVIEW

Review of plasmonic fiber optic biochemical sensors: improving the limit of detection

Christophe Caucheteur · Tuan Guo · Jacques Albert

Received: 6 October 2014 / Revised: 2 December 2014 / Accepted: 12 December 2014 / Published online: 24 January 2015

Abstract This paper presents a brief overview of the technologies used to implement surface plasmon resonance (SPR) effects into fiber-optic sensors for chemical and biochemical applications and a survey of results reported over the last ten years. The performance indicators that are relevant for such systems, such as refractometric sensitivity, operating wavelength, and figure of merit (FOM), are discussed and listed in table form. A list of experimental results with reported limits of detection (LOD) for proteins, toxins, viruses, DNA, bacteria, glucose, and various chemicals is also provided for the same time period. Configurations discussed include fiber-optic analogues of the Kretschmann–Raether prism SPR platforms, made from geometry-modified multimode and single-mode optical fibers (unclad, side-polished, tapered, and U-shaped), long period fiber gratings (LPFG), tilted fiber Bragg gratings (TFBG), and specialty fibers (plastic or polymer, microstructured, and photonic crystal fibers). Configurations involving the excitation of surface plasmon polaritons (SPP) on continuous thin metal layers as well as those involving localized SPR (LSPR) phenomena in nanoparticle metal coatings of gold, silver, and other metals at visible and near-infrared wavelengths are described and compared quantitatively.

Published in the topical collection *Direct Optical Detection* with guest editors Guenter Gauglitz and Jiri Homola.

C. Caucheteur
Electromagnetism and Telecommunication Department, University of Mons, Boulevard Dolez 31, 7000 Mons, Belgium

T. Guo
Institute of Photonics Technology, Jinan University, 601 Huangpu Road West, Guangzhou 510632, China

J. Albert (✉)
Department of Electronics, Carleton University, 1125 Colonel By Drive, Ottawa K1S 5B6, Canada
e-mail: Jacques.albert@carleton.ca

Keywords Plasmonics · Polaritons · Photonics · Optical fiber · Grating · Bragg · Chemical sensing · Biochemical sensing · Immunosensing · Gold · Nanoparticles

Introduction

The purpose of this paper is to review advances in optical-fiber-based, label-free direct detection devices using surface plasmon resonance (SPR) effects. Throughout the paper, but apart from context-specific instances, the SPR acronym will be used both for devices involving surface plasmon polaritons (SPP) along metal surfaces and for localized SPR (or LSPR) which refers to three-dimensional plasmon resonances in metal particles. Furthermore, SPR is meant here in its broadest possible sense, i.e., for the measurement of the properties of light waves interacting with nanoscale metal particles or films [1–3]. Using such resonances in sensing has been the object of much research, dating back over 20 years, as reviewed elsewhere [4–8]. More specialized reviews dealing with fiber-based SPR sensors also appeared up to five years ago [9, 10]. Based on these pioneering investigations, research in the last few years has led to notable advances. These advances go beyond laboratory proof-of-principle experiments and report impressive limits of detection (LOD) in real-life applications, using both conventional configurations and new device geometries. It was therefore felt that a critical survey of recent developments would be useful at this time so that research groups and user communities could get a good understanding about the performance of current technologies and methods as well as about the potential of the newer ones.

The rapid and accurate detection of analytes in small concentration (proteins, ADN, pathological markers, toxins etc.) is crucial in numerous fields such as medical diagnosis, environmental monitoring, or quality control in the food industry.

In the context of these applications, detection systems can be divided into two general categories: laboratory-based and field-based systems, where "field" is taken to mean detecting in samples where they happen to be located in contrast to having to bring samples back to a laboratory. A further distinction can be made between direct detection and labeled method, whereby the latter requires some sort of tag added to the analyte in order to enable its detection. Direct detection methods are generally preferred over labeled approaches from the point of view of cost and ease of use (and for field use in particular), but direct detection is also generally less sensitive because labeling enables the use of additional selection and amplification methods that raise the signal level of very small concentrations over the background response of samples.

The use of optical-fiber devices as sensors presents many well-known desirable features (size, cost, light path control) for both labeled and label-free methods but those advantages are best expressed in label-free solutions as they contribute to the overall reduction in costs and ease of use factors [11, 12]. Fiber-optic sensors can be inserted into the media to be sensed (instead of having to bring samples inside an instrument) either as a hand-held probe or as a set of remotely operated devices along a fiber-optic cable (in environmental monitoring applications for instance). Of course, fiber-based sensing solutions are not competitive with bulk optic laboratory instrumentation (like microplate array systems) in applications such as pharmaceutical research where a large number of tests need to be performed simultaneously in parallel. However there appears to be interesting niche applications where fiber sensors' potential low cost and ease of use could lead to widespread deployment, such as screening for viral or bacterial infections, checking for specific toxins in food processing plants, and monitoring the water quality in urban water supply systems or in the environment surrounding toxicogenetic industries and resource extraction operations.

The current review describes results obtained since the mid-2000s, and covers advances in sensor design, sensor interrogation techniques, surface functionalization, and the use of either custom designed or mass-produced conventional fibers in sensor fabrication. Among the many interesting developments that occurred, the most notable feature has been the demonstration of LODs that approach those achieved using much larger, costlier, laboratory tools. These achievements are the results of improvements in instrumentation, fibers, coatings, and coating characterization tools, and also in our theoretical understanding of plasmonic interactions between light waves, metals, and dielectrics at the nanoscale, which in turn allow for better data analysis techniques.

Following a brief introduction about the theoretical underpinnings of fiber SPR devices, the paper is organized around a classification according to device geometry (whole fiber, modified fiber, custom designed fiber), to the "kind" of plasmonic interaction (excitation of SPPs in continuous thin metal layers, excitation of LSPRs in nanoparticles), and to the interrogation technique (mainly spectral absorption and grating-assisted mode coupling, as well as multimode vs single-mode fibers). A general survey of the literature is presented in table form where the main characteristics and performance indicators of representative reported results are given. Those performance indicators include the bulk refractometric sensitivity, which indicates how the device responds to changes in its environment and is usually the first metric used to predict the performance of (bio)chemical sensors. However, refractometry is definitely not the main purpose of SPR sensors and the last section presents another group of publications that report on the performance of fiber SPR devices in actual applications, as measured by their experimentally determined analyte LODs. The most striking finding is that widely different approaches, from the "standard" cladding-removed, gold-coated multimode fiber with spectral interrogation, to very sophisticated, nano-patterned customized fiber design, with grating-assisted devices in between, are all able to achieve impressive LODs. This is likely because the most important factors in lowering the LOD and increasing the specificity in label-free detection lie in the noise properties of sources and detectors [13], as well as in the quality of the surface functionalization, where great advances have been made over the last few years [14, 15].

SPR generation on optical fibers

Surface plasmon polaritons (SPP)

The most common approach to excite surface plasmon waves on thin metal films is the Kretschmann–Raether configuration sketched in Fig. 1 [2]. In this approach, light is injected through a prism towards a plane face coated by a thin layer of noble metal. The incidence angle at the glass–metal

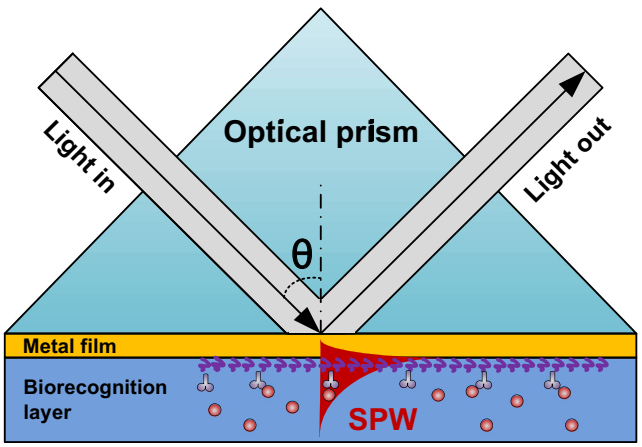

Fig. 1 Sketch of the operating principle of the Kretschmann–Raether prism (*SPW* surface plasmon wave)

interface is chosen to be larger than the critical angle so that light is totally internally reflected. The evanescent wave associated with the total reflection propagates along the glass–metal interface and can transfer energy to an SPP of the opposite metal-surrounding medium interface when its propagation constant (parallel to the metallic surface) equals that of the SPP. In this configuration, such SPP can only occur at the external surface of the metal film because its propagation constant is too large to allow for radiation there. On the inner metal surface, a radiative wave exists and the tangential component of its propagation constant is necessarily too short to excite the SPP of that interface. The other condition necessary for the excitation of the SPP wave is that the polarization of the light must be perpendicular to the metal surface, i.e., TM-like. Since the SPP has a single well-defined propagation constant that depends only on the permittivities of the metal and of its surroundings, there are only certain combinations of wavelength and incidence angle that can excite the SPP. Such excitation corresponds to a transfer of power from the incident light beam and it is revealed by detecting a decrease in the reflected power. In sensing applications where the Kretschmann–Raether prism is used to measure the permittivity of the surrounding medium (or the effect on permittivity of material and molecules attached to the surface), three methods can be used to measure the SPP resonance condition and its changes. Angular interrogation consists of using monochromatic light and precisely scanning incidence angle values above the critical angle. In spectral interrogation the incidence angle is fixed and a broadband or tunable light source is used to detect resonances. Finally, the relative phase shift between TE and TM incident light as a function of wavelength or angle can also be used [16]. The surface plasmon resonance condition thus measured is strongly sensitive to surrounding refractive index (SRI) changes, and it is used in practice to measure density fluctuations, thickness changes, and molecular adsorption when bioreceptors are anchored on the metallic surface.

Localized surface plasmon resonances (LSPR)

In contrast to SPP that are lossy waves propagating along continuous metal surfaces, the LSPR is an optical phenomenon generated by light waves trapped within conductive nanoparticles (NPs) with dimensions smaller than the wavelength of light. It results from the interaction between the incident light and electrons in the conduction band of the metal [17]. This interaction produces coherent localized plasmon oscillations with a resonant frequency that strongly depends on the composition, size, geometry, dielectric environment, and particle-to-particle separation of the NPs. Commonly used materials for NPs are noble metals such as Ag and Au, which exhibit LSPR in the visible range of the spectrum. The detection of LSPR for sensing consists of measuring changes in the absorption spectra of broadband light waves moving through NP dispersed in liquids or deposited on solid substrates. Similar to SPP, the LSPR is revealed by an increase in absorption at a certain wavelength, and this wavelength changes when the immediate vicinity of the NPs is modified. One significant difference between SPR and LSPR is that the use of NPs can lead to much increased surface contact area compared to continuous thin films, thereby providing more opportunity for small concentrations of analytes to bind to the metals and modify the measured resonances.

Optical fiber implementations of surface plasmon sensors

Plasmonic optical fiber sensors constitute miniaturized counterparts to bulky prisms and microscope systems used to probe SPR and LSPR. They allow remote and real-time operation in microfluidic chambers and they have the potential for in vivo measurements. However optical fibers are designed to guide light with as little loss as possible and are therefore constructed in such a way that light gets totally internally reflected at an internal interface, i.e., at the boundary between a core and a layer of cladding that prevents light from reaching the surroundings. So in order to use fiber-guided light to interact with metal coatings or particles and excite plasmonic resonances, the light path must be interrupted or modified. The early fiber optic SPR sensors were based on structures where the cladding was removed to expose the core surface but many other configurations have emerged since then. In all cases, spectral interrogation is used (whether through conventional absorption or reflection spectrum measurement or by measuring changes in the transmission or reflection of a narrowband light beam with a wavelength located on the shoulder of an SPR resonance). Finally, some configurations use a "doubly resonant" system where a natural system resonance (that of a grating for instance) is perturbed by the presence of an SPR or LSPR.

On light polarization in plasmonic optical fiber sensors

It was mentioned in "Surface plasmon polaritons (SPP)" that the excitation of SPP required the light to be TM polarized, i.e., perpendicularly to the metal surface. This is obviously an issue for cylindrical fibers since fiber modes are generally hybrid with spatially varying three-dimensional electric fields. The consequence of this is that only part of the light internally reflected at the exposed core boundary is of the correct polarization state and therefore the maximum attenuation possible is of the order of 50 % (for unpolarized or randomly polarized light). This issue cannot be overcome by the use of polarization-maintaining fiber since linearly polarized light is only perpendicular to the metal surface along two diametrically opposed locations. However, mechanically polished fibers with a D-shape structure do have a flat metal surface and their response can be optimized with properly oriented

incident linearly polarized light. A notable exception to this issue will be mentioned in the context of tilted fiber Bragg grating (TFBG) sensors, where the selective excitation of cladding modes with almost 100 % radially polarized light at the cladding surface is possible. Finally, polarization is normally not a concern for LSPR-based sensors because of the three-dimensional nature of the metal surfaces.

It is the main purpose of the present paper to review recent advances in fiber SPR sensors based on these geometries. The most relevant configurations can be classified into three categories. They are summarized in "Recent fiber optic SPR sensors" while their main performance indicators are presented in Table 1.

The main performance indicators for plasmonic biochemical sensors are their sensitivity, accuracy, repeatability, and LOD. The sensitivity is the ratio of the change in the sensor output (e.g., wavelength, amplitude, angle of incidence) versus change in the measurand (e.g., density, thickness, analyte concentration). The accuracy defines the degree to which the sensor readout value corresponds to the actual value of the measurand. The repeatability refers to the sensor ability to reproduce the same response under the same stimulus over many repetitions. Finally, the LOD corresponds to the lowest concentration of analyte that the sensor is able to detect (above the measurement noise). When comparing the sensor performances from one configuration to another, it is insufficient to compare only sensitivities (i.e., wavelength shifts), without considering the wavelength measurement accuracy. It is therefore more convenient to refer to the figure of merit (FOM) of the device. The FOM is proportional to the ratio between the wavelength shift sensitivity and the linewidth of the resonance, taking into account that it is easier to measure the exact location of a narrow resonance than a broad one [18].

Recent fiber optic SPR sensors

Geometry-modified fibers

This first category groups plasmonic optical fiber sensors based on a modification of the optical fiber that brings the core-guided light in direct contact with the surrounding medium, and where the SPR response is obtained from the transmission spectra. The most straightforward configurations consist in removing the cladding entirely or in part, via a chemical etching process or by side-polishing, as sketched in Fig. 2 [19–27]. Such unclad or D-shaped sensors are most often used at operating wavelengths between 500 and 800 nm and in recent years unclad sensors have been made from very large core fibers, in the range from 200 μm and 600 μm instead of small core single-mode fibers, such as those used in communication systems, because cladding removal alters the mechanical resistance of pristine fiber surfaces [19, 21]. Another variant on the same approach consists of making a narrow trench in the cladding with a femtosecond laser source, thereby exposing a narrow strip of the core, where NPs can be deposited to form an LSPR sensor [27]. It is worth mentioning that wavelength interrogation of SPR usually requires a fixed incidence angle to be effective, otherwise there are many combinations of wavelength and angle that satisfy the phase-matching condition for the excitation of the SPP. In these

Table 1 Summary of the best experimental performances for fiber optic plasmonic refractometers

Sensor configuration	Wavelength range	Ultimate bulk refractometry	Figure of merit	Reference
I. Geometry-modified fibers				
Unclad/etched fiber	500–800 nm	ca. 4,000 nm/RIU	ca. 40	[19–22]
Side-polished/D-shaped fiber	500–800 nm	ca. 3,200 nm/RIU	ca. 64	[23–27]
Tapered fiber	500–800 nm	ca. 11,800 nm/RIU	ca. 118	[28–34]
Hetero-core structure	500–800 nm	ca. 5,000 nm/RIU	ca. 33	[35, 36]
U-shaped fiber	500–800 nm	ca. 30 ΔA/RIU	N/A	[37]
Arrayed fiber end face	500–1,600 nm	ca. 120 nm/RIU, ca. 17 ΔI/RIU	ca. 1	[38–41]
II. Grating-assisted fibers				
LPFGs	800–1,200 nm	ca. 10 ΔT/RIU	N/A	[44]
TFBGs	1,500–1,600 nm	ca. 500 nm/RIU	ca. 2,500	[46, 50–52]
III. Specialty fibers				
Polarization maintaining	ca. 800 nm	ca. 3,200 nm/RIU	ca. 40	[54]
Microstructured	500–800 nm	ca. 6,430 nm/RIU	ca. 90	[55–62]*
Polymer	700–800 nm	ca. 1,300 nm/RIU	ca. 9	[63–65]

ΔA/RIU absorption change per refractive index unit, *ΔT/RIU* transmission change per refractive index unit, *ΔI/RIU* intensity change per refractive index unit, *N/A* not applicable

*Only theoretical values

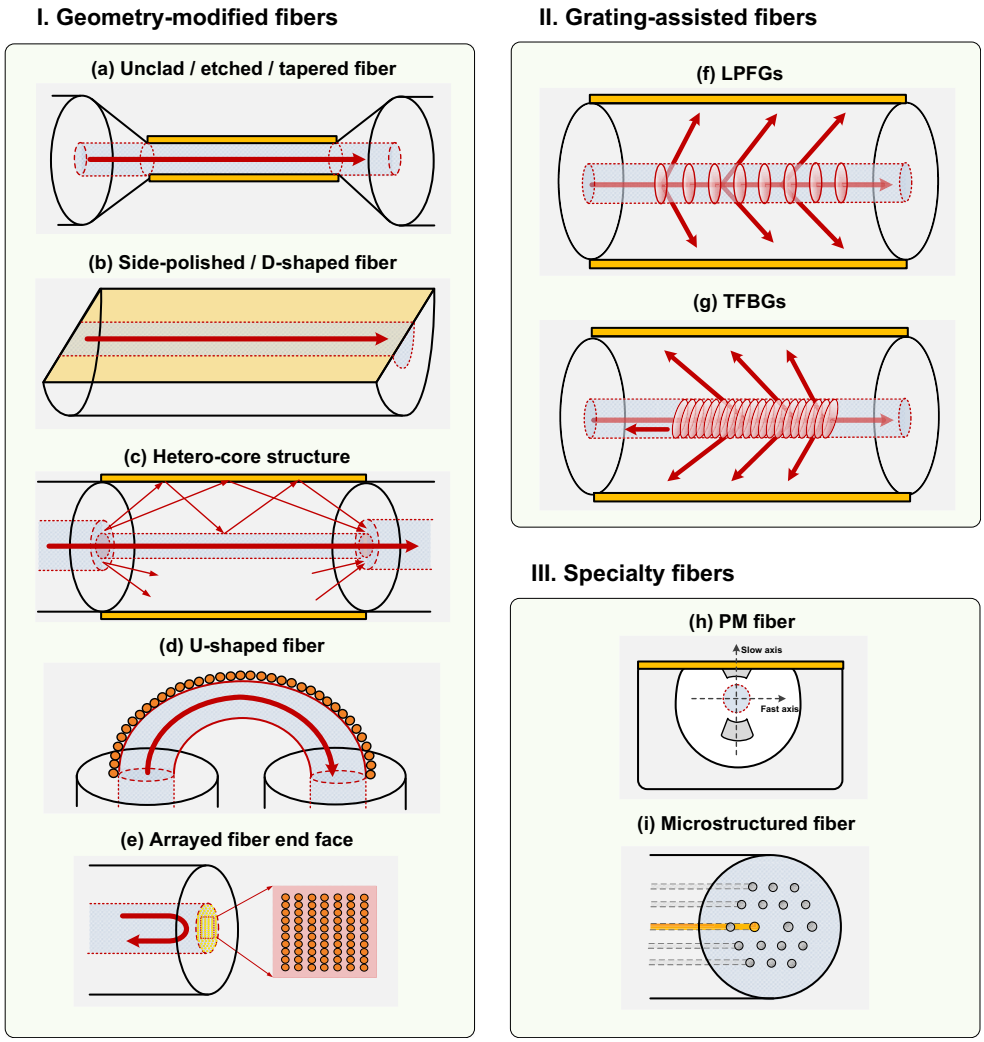

Fig. 2 Sketch of the different fiber-optic SPR configurations. *I* geometry-modified optical fibers: **a** unclad/etched/tapered fiber, **b** side-polished/D-shaped fiber, **c** hetero-core structure, **d** U-shaped fiber, **e** arrayed fiber end-face; *II* fiber gratings: **f** LPFGs, **g** TFBGs; *III* specialty fibers: **h** PM fiber; **i** microstructured fiber

conditions the measured resonance would be washed out. However, even in large core multimode fibers light propagates within a relatively narrow range of incidence angles at the core boundary which results in well-defined SPR spectra. The full width at half maximum (FWHM) of the typical resonances in the transmitted amplitude spectrum lie between 50 and 100 nm, while the ultimate refractometric sensitivity can reach 4,000 nm/RIU (RIU, refractive index unit).

Another group consists of tapered fibers that are produced by gently stretching along the propagation axis while heating over a flame or heated filament, such that the glass becomes soft. This procedure makes optical fibers thinner over some length, typically a few millimeters or centimeters. The fiber core also gets thinner by the same factor as the total fiber and eventually the evanescent wave from the core reaches the outer surface and is exposed to the surrounding medium. An SPR sensor results when a metallic layer is placed over the tapered region [28–34]. The ultimate refractometric sensitivity of such structures reaches 12,000 nm/RIU [29].

Other configurations, so-called hetero-core structures, are realized by splicing two different kinds of optical fibers (Fig. 2c). The most often encountered scheme consists in splicing a single-mode fiber (SMF) section between two multimode fibers (MMFs) [35, 36]. The core mismatch between the fibers used causes the core-guided light in the MMF to couple to cladding modes in the SMF section prior to again being recaptured by the exit core. This configuration would work with just about any combination of mismatched fibers but the one reported here (MMF–SMF–MMF) is quite likely the most efficient in terms of power budget and overall cost because the input and ouput fibers have the largest core and hence capture much of the cladding mode light from the middle section. As in previous cases, plasmonic interactions occur at the outer surface of the SMF (i.e., of the "middle" fiber) when it is surrounded by a metal layer. The refractometric sensitivity of hybrid SMF–MMF sensors can reach 5,000 nm/RIU.

All of the aforementioned configurations require measurements of transmitted light, but for practical reasons (the

frequent need for single-ended probes having a common input and output path) they are often adapted to work in reflection as well. For operation in reflection mode, the fiber is cleaved right after the sensing region and coated with a reflective layer (most often the same as the one used for plasmonic generation). As a result the transmitted light is reflected towards the input, and a side benefit is that it goes through the sensing region twice, thereby amplifying the response to the coating and its environment.

The most non-intrusive approach to extract light from a fiber core is quite likely by bending. It is well known that optical fibers become lossy when bent beyond a certain critical radius, because the evanescent field associated with total internal reflection becomes radiative (i.e., a cladding mode in a clad fiber). Therefore, fiber SPR devices can be obtained using metal-coated U-shaped optical fibers, as sketched in Fig. 2d. While a reversible bend obtained by flexing the fiber would work, it would not be very reliable since the outer glass surface of the bend would be under very strong tensile stresses. Therefore, it is preferable to fabricate a permanent sharp bend in a fiber. The structures demonstrated so far are obtained from large core fibers by exposing an unclad section to a flame (from propane or oxy-butane torch or even a simple wax candle) and shaping it to form a U. By controlling the heat, it is possible to realize different bend radii with good repeatability, down to 0.5 mm. U-shaped optical fibers are intrinsically single-ended because the input and output fibers can be co-located in a very small tube, even if they operate in transmission. The example reported here uses NPs for LSPR generation [37]. In this case, the transmitted amplitude spectrum contains a resonance band whose amplitude can be tightly correlated with the SRI value.

Finally, there is an important subset of single-ended intrinsic fiber optic sensor probes that has been the object of renewed interest owing to advances in nano-patterning technologies. It consists of fiber sensors where the sensing surface is located on the end of a cut fiber. The current review does not include fiber sensor devices where the fiber is just used to bring pump light to a medium and to recover fluorescence or Raman signals for instance. However, as illustrated in Fig. 2e, (L)SPR sensor probes have been developed by patterning the flat fiber end face or covering it with an array of NPs [38–41]. The core-guided light is in this case directly exposed to the NPs, yielding LSPR generation. Most often, this is carried out on standard optical fibers that reflect light back towards a detector through a splitter at the input end. Different strategies can be exploited here. Nguyen et al. [38] made an array of apertures in a metal film deposited on the cleaved end face of the optical fiber, while Lin et al. [41] used the e-beam lithography nano-fabrication process to pattern gold nano-dot arrays directly on the end face. Also, depending on the realization of the probe, the interrogation is either based on the monitoring of a wavelength shift of the reflection band or intensity changes. The refractometric sensitivity can reach 196 nm/RIU.

Grating-assisted fibers

Instead of removing part of the cladding to access core-guided light, gratings photo-inscribed in the core can be used to diffract some of the light into the cladding. There are two advantages to this approach: the mechanical resistance of the fiber is minimally impacted and grating coupling is a resonant phenomenon that only occurs at specific wavelengths in guided configurations (i.e., different fiber modes couple at different wavelengths). This is equivalent to a coupled resonator system where the grating couples two fiber modes with each other and the metal film couples a fiber mode to an SPP. When the two resonances overlap, the grating resonances become sensitive to the changes in the SPR. Conventional short period (submicron) fiber Bragg gratings (FBGs) are narrowband, wavelength-selective filters that couple the forward-propagating core mode to a backward-propagating one. However, light remains confined in the fiber core and is therefore insensitive to changes in the surrounding medium. Etched FBGs with the cladding removed by immersion in an acid solution have thus been proposed for sensing purposes [42, 43]. More advantageously, “radiating” gratings couple light from the core towards the cladding while preserving the mechanical integrity of the optical fiber. Two well-known configurations have been demonstrated for this purpose. Long period fiber gratings (LPFGs) have refractive index modulation periods that are typically between 50 and 500 μm (or 1, 000 times larger than those of FBGs). They couple the forward-going core mode into forward-going cladding modes (Fig. 2f) and present a transmitted amplitude spectrum featuring several broadband resonances (FWHM ca. 20–50 nm) in a spectral range of a few hundred nanometers. Plating the fiber cladding surface with a metal layer, as done by Schuster et al. [44], enables the coupling of the cladding mode to an SPP and the measurement of changes at the metal surface by monitoring the LPFG resonance. The other configuration uses TFBGs that have grating fringes slightly angled with respect to the perpendicular to the optical fiber propagation axis (Fig. 2g). Two kinds of coupling take place in these structures: the self-backward coupling of the core mode and the backward coupling of the core mode with tens to hundreds of cladding modes within the same spectral window of 100 nm or so. The TFBG resonances result in a dense comb-like transmitted amplitude spectrum featuring narrowband cladding mode resonances (FWHM ca. 100 pm) on the short wavelength side of the Bragg (core mode) resonance, as shown in Fig. 3 [45]. One of the most important features of the TFBG spectrum is the presence of the Bragg resonance that is immune (in wavelength and power) to the external medium and that can further

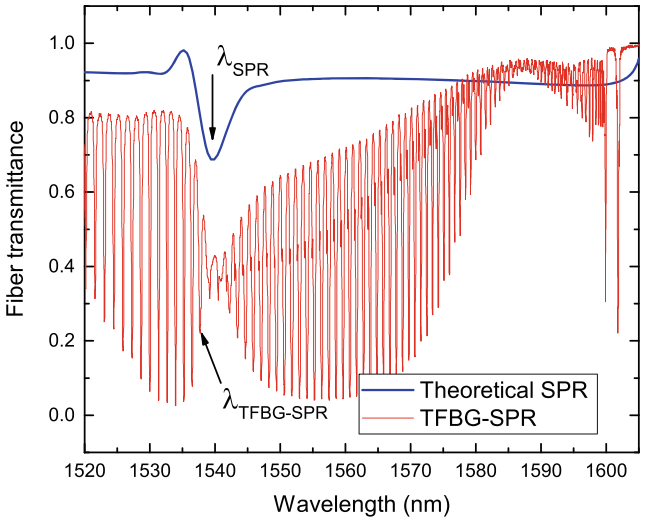

Fig. 3 Comparison between the best theoretical SPR response for 50-nm gold on silica in the Kretschmann–Raether configuration (*thick blue line*) and a measured TFBG-SPR spectrum with the same thickness of gold (*thin red line*). The *arrows* indicate the resonance to be followed in each case

be advantageously used to de-correlate unwanted temperature and power level fluctuation effects from the sensor response. Similar to LPFGs, plasmon generation is achieved when a metallic overlay is deposited on the cladding surface [46]; but unlike LPFGs, only a subset of the cladding mode resonances are phase matched to the SPP, i.e., those that have effective indices close to that of the SPP at the outer boundary of the metal coating. Differential measurements between SPP-matched cladding modes and those that are not matched can be used to improve measurement accuracy. A final important feature of TFBGs is that the tilt of the grating planes breaks the cylindrical symmetry of the fiber and that as a result the resonances corresponding to higher-order cladding modes (i.e., those which are phase matched to SPPs of a gold–water interface for instance) can be excited separately for modes that have radially polarized and azimuthally polarized electric fields [47]. Therefore, the use of radially polarized resonances allows for the excitation of SPPs while neighboring azimuthally polarized ones are actually shielded from the surroundings by the metal films [48, 49]. This effect has been used to develop fiber SPR refractometric sensors with SRI sensitivities of ca. 500 nm/RIU [46, 50–52], and biochemical sensors that will be described in "Applications". Finally, the differential refractometric sensitivity of the polarized cladding modes of TFBGs has also been shown to increase with the deposition of sparse layers of high aspect ratio nanowires with a broad LSPR response in the near infrared [53].

Specialty fibers

This last category groups non-conventional optical fibers. Among those are polarization-maintaining fibers that were used in a side-polished configuration to expose the core-guided mode to the surrounding medium [54]. Polarization-maintaining optical fibers support two orthogonal nearly linearly polarized modes ("slow" and "fast" polarizations). When one of the birefringence axes of the fiber is precisely aligned with the gold film, the corresponding polarization excites the surface plasmon wave (Fig. 2h). This configuration intrinsically overcomes the potential problem of fluctuations in the polarization of light interacting with surface plasmons (e.g., due to optical fiber deformations) that can produce unwanted fluctuations in the sensor output. In SMFs, this issue is alleviated in practice by using depolarized light. Polarization-maintaining fibers present a similar refractometric sensitivity as SMFs, roughly 3,200 nm/RIU.

Microstructured optical fibers guide light using air tunnels or longitudinally invariant refractive index structures that surround a hollow or solid glass core. Different configurations (multi-hole, three-hole, "grapefruit", etc.) were proposed for plasmonic generation by coating the core or the other holes with NPs, over the last millimeters or centimeters of the fiber, or by filling some of the holes with metal [55–62]. In all cases, the guiding geometry must be such that some part of the guided light (usually the evanescent tail of guided modes) interacts with a metal surface along part of the length only (otherwise there would be too much loss and no light would reach the detector). In this group, only three studies [57–59] report on fabricated devices with metal layers for exciting SPR but no sensing results. Wong et al. [60] do present sensing results but the microstructured fiber is only used to provide a mismatched core in a hetero-core approach. On the theoretical side, various performances were computed for microstructured fibers with metal inclusions or layers, yielding ultimate predicted refractometric sensitivities equal to 6,430 nm/RIU for a D-shaped microstructured fiber in which the central core is filled with liquid and its center located 2.6 μm from the flat surface where a 40-nm layer of gold is placed [55].

Finally, plastic optical fibers (POFs) based on poly(methyl methacrylate) (PMMA) (step-index [63, 64] and microstructured [65]) have been used for plasmonic generation. The core-guided light has been exposed to the surrounding medium by an etching or a side-polishing process. The performances reported so far are slightly inferior to those obtained for silica optical fibers but plastic optical fibers bring additional assets such as improved biocompatibility.

The ultimate performances of all these configurations are reported in Table 1. In terms of experimentally demonstrated FOM, TFBG-based SPR sensors surpass all other configurations by more than one order of magnitude. As shown in Fig. 3, this results from the fact that they exhibit narrow resonance bands (FWHM ca. 0.1–0.2 nm) compared to even the best possible theoretical value (ca. 5 nm obtained by calculating the reflection from the base of a prism in the

Kretschmann–Raether configuration), also keeping in mind that the experimental SPR FWHM from other fiber configurations all exceed 20 nm and more as reported in "Geometry-modified fibers".

Finally, a short comment about the nature of the metals used in fiber SPR and LSPR technologies. Thin noble metal sheaths can be successfully deposited on optical fibers using well-established technologies, such as electroless deposition, electroplating, or sputtering [66]. The last of these is used more routinely and provides very high quality metal surfaces. To promote adhesion, a 2- to 3-nm buffer layer of chromium or titanium is often sandwiched between the optical fiber surface and the gold coating. Another option consists in thermally annealing the gold coating, which modifies its morphology and ensures robustness [67]. What is important to realize is that it is quite difficult to obtain very uniform metal layers at the thicknesses required for optimum SPR excitation (around 50 nm), and as a result that there may be some rugosity, or particles forming instead of smooth layers. This will have an effect on the SPR properties because the effective complex permittivity of the metal layers will be different from that of the bulk values (which are often used in the design of the sensors) [68–70]. A major recent development on the materials side relates to the use of non-metal layers for plasmonic applications, such as certain types of semiconductors and oxides, as reviewed recently [71]. These materials have yet to be explored in fiber-based systems but represent interesting avenues of research to pursue further.

So the regime of very thin metals tends to morph into that of metal NPs, more suitable for LSPR operation. However, NPs are most efficiently prepared using specific techniques. It is possible to pattern metal NPs on fiber surfaces using lithographic or nanostamping tools, but in general metal NPs are synthesized from solution and attached chemically to fiber surfaces that have been prepared for this purpose to form strong covalent bonds. Such solution-based processes tend to be economical and scalable for mass production. Metal NPs are now available commercially in various shapes and sizes, thereby lowering the entry threshold for researchers in photonics wanting to develop LSPR-based sensors. As illustrated in Table 2, most LSPR sensors operate at visible wavelengths because metal NPs have strong resonances in this part of the spectrum. However, some results were obtained in the near infrared, with nanowires (in which a broad absorption associated with the long axis of the wires resonates at longer wavelengths), and in some of the application papers listed in "Applications".

To conclude this section, some indications about how the best detection results can be achieved are now provided:

- Enhancing light-coupling mechanisms from the fiber core to the immediate surroundings of the cladding. This arises by increasing the operating wavelength, inducing a higher penetration depth of the electromagnetic field (evanescent wave) in the surrounding medium.
- Optimizing the spectral resolution (favoring narrow resonance bands over broad ones) also improves the overall FOM and hence the LOD. Among all plasmonic optical fiber configurations reported, TFBGs operating in the near-infrared probe the surrounding medium over a few hundred nanometers with narrow resonance bands whose evanescent field has the correct polarization.
- Amplifying the SPR response with smart labeling techniques using gold, silica, and/or magnetic nanoparticles. Nanoparticles improve the sensitivity not only because of an increased binding mass but also an increased perturbation of the evanescent electromagnetic field. Hence, with their different sizes and shapes, they can be functionalized with different bioreceptors (antibodies, aptamers, etc.) to realize "sandwich-like" bioassays. There is a strong confinement (that arises from the excitation of LSPRs) of the electromagnetic field, which is favorable for its interaction with analytes.
- Improving the SPR response by nano-patterning the gold sheath, yielding similar effects as those obtained from NPs. It must be pointed out here that the patterning or distribution of nanoparticles need not be periodic, or regular in any way, as most fiber optic probes measure the average perturbation of the light over macroscopic distances along the fiber (several millimeters at least).

Applications

This section begins with an overview of available techniques to bind biomolecules on gold surfaces (the most common substrate layer for SPR sensors). Then, it focuses on prominent examples of biochemical applications based on plasmonic optical fiber sensors.

Molecules commonly used as bioreceptors grafted on the gold surface are immunospecies (antibodies, antigens), enzymes, nucleic acids (DNA, RNA), and cells. Antibodies possess reaction sites capable of recognizing a very specific target analyte, i.e., the corresponding antigen. Plasmonic sensors relying on antibody–antigen affinity measure refractive index changes induced by the adsorption of antigens by grafted antibodies. Enzymes are biologic catalysts that can accelerate up to 10 million times the chemical reactions occurring within or around cells. When used in a plasmonic configuration,

Table 2 Refractometric performance of LSPR-based optical fiber sensors

Type of NPs	Sensor configuration	Wavelength range	Bulk sensitivity	Ref.
Au NPs	Unclad MMF	600 nm	471 nm/RIU	[72]
Au NPs	Hetero-core (PCF-MMF)	530 nm	−731 %/RIU	[73]
Au nanodots	Fiber end face	630 nm	195.72 nm/RIU	[74]
Au nanospheres	Fiber end face	555 nm	387 nm/RIU	[75]
Ag nanospheres	Fiber end face	425 nm	N/A	[75]
Ag nanowires	TFBG	1,550 nm	650 nm/RIU	[53, 76]

the product of the chemical reaction catalyzed by enzymes changes the sensor response. DNA molecules consist of double-stranded helices that contain all the information required for the synthesis of proteins. The two strands making up a DNA molecule can be separated but they will only recombine with their exact matching sequence, a process called hybridization that is often used in biomedical sensors. After grafting a single strand of DNA corresponding to the desired sequence on the sensor surface, the operating principle is based on monitoring for the occurrence of an interaction between the DNA strands and their complement, as evidenced by a thickening of the grafted layer when it occurs. Finally, entire cells can also be attached to fiber SPR sensors. In this case, cell metabolism can be monitored via indirect means that have an impact on the density of the cells and on their distribution along the fiber surface (for instance healthy cells can grow and multiply, thereby increasing locally the refractive index, while dying cells can fall off the fiber surface).

The simplest method to use receptor biomolecules on fibers is by direct (physical) immobilization on gold substrates through adsorption (ions exchange, van der Waals interactions, hydrogen bonds). While the physical mechanisms involved in this case are not fully understood, it is thought that hydrophobic interactions dominate the immobilization process [77]. This process is rarely used as it suffers from considerable practical drawbacks such as lack of reproducibility of the receptor binding and non-specificity of the detection. These limitations are overcome by exploiting engineered strong covalent bonds between receptors and the sensor surface using functional groups. Two strategies are available for covalent immobilization:

– *One-step receptor immobilization*. Existing functional groups within the receptor biomolecules are exploited or modified to allow for the formation of a self-assembled monolayer (SAM) of amphiphilic molecules on the gold surface. SAM reagents are usually composed of long alkyl chains, yielding a stable, dense, and ordered assembly driven by intermolecular hydrophobic interactions. Covalent bonds between gold and sulfur, usually mediated by the sulfhydryl (SH) radicals in thiols, are most often used in practice. Other configurations use carboxyl radicals (COOH), amine (NH_2), or hydroxyl radicals (OH).
– *Two-step receptor immobilization*. Here, the gold surface is first modified with a bifunctional SAM that further reacts with functional groups on receptor biomolecules. Bifunctional molecules have thiol groups at one end and other functional groups at the other end to make a surface reactive to specific targets. The intermediate organic layer helps to preserve the specific recognition properties of the receptors by removing the need to have the receptor also bound to gold. This intermediate layer can be a SAM or a composition of a SAM and a polymer film.

Indeed, the transducer surface can be modified by polymer grafting. For instance, the “grafting from” technique allows great control over the thickness of the polymer film. It consists of immobilizing an initiator on the surface and then growing the polymer chains from monomers present in solution around the surface. After the immobilization of the polymer film of a desired thickness is completed, this film can be used to graft biomolecules with help from reactive functional groups or coupling molecules.

Finally, the substrate functionalization can also be initiated by the deposition of a multilayer of polyelectrolytes, obtained by successive adsorptions of oppositely charged polyelectrolytes (layer-by-layer deposition).

Hence, as summarized in Fig. 4, a typical plasmonic optical biochemical sensor is obtained from four main complementary steps:

1. Fiber modification to bring the evanescent light wave from the guided light in contact with the surrounding medium
2. Deposition of a thin metal layer for SPR generation
3. Functionalization of the metal surface
4. Grafting of receptor molecules

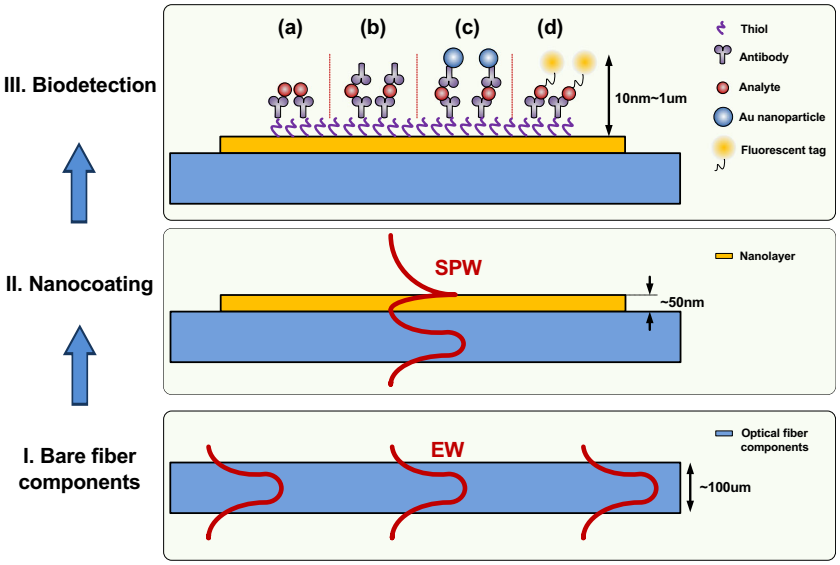

Fig. 4 Fiber-optic SPR biosensors fabrication process: *I* bare fiber components, *II* fiber surface coating with nano-layer, *III* bio-sample detection: **a** direct detection; **b** sandwich assay; **c** sandwich assay amplified with Au nanoparticle; **d** sandwich assay with fluorescence tag. (*EW* evanescent wave, *SPW* surface plasmon wave)

Following step 4, as shown in Part III of Fig. 4, various techniques can be implemented to increase the sensors response to the binding event between the receptor and its target analyte, such as additional molecules, NPs, or fluorescent tags. However these fall outside of the scope of this special issue on direct detection methods as they involve tagging of the targets.

Table 3 presents some of the experimental results reported in the literature for plasmonic optical biochemical sensing. It provides details of the type of sensor and excitation used, the functional materials and analyte investigated, and the claimed sensor performances. While most of the results presented refer to detection in aqueous solutions, the last few entries deal with SPR-assisted gas-phase detection of chemicals [100–103]. A few of the references also report on LSPR implementations using nanodisks, cages, "dots", and spheres on fibers: these use mostly the optical field enhancement near the NP surface associated with plasmonic resonances at visible wavelengths to become sensitive to small molecular binding events on the NPs. However it has also been demonstrated that it is possible to obtain much improved LODs at near-infrared wavelengths that are far from the LPSR of the particles [98]. In this case, the LOD improvement is attributed to the use of polarized cladding modes in a grating-assisted fiber device that are strongly perturbed by NPs. It is also notable that this improvement was achieved in spite of a significant decrease in the sensitivity slope.

Table 3 confirms that there is no universally accepted method to characterize sensor performances since some papers present only figures about sensitivity (S) and resolution while others provide the LOD for the analyte investigated. In spite of this, the numbers still indicate that the performances of the most recent fiber-based SPR biochemical sensors begin to be comparable to those obtained using standard, bulkier, and costlier prism-based readout systems. Again, there should be application niches where the LODs reported are sufficient, such as controlling epidemics and screening for specific pathologies in large populations, and where the relative low cost and instrument portability would be strong assets. So far, however, despite all efforts that have been conducted in developing plasmonic optical fiber sensors, the technology is still far from being mature and examples of its use in complex (bio)chemical applications remain limited, even if the technology clearly possesses the potential to be used in situ or even possibly in vivo. With these applications in mind, the most straightforward configuration remains undoubtedly based on unclad fiber. If this is implemented using telecommunication-grade optical fibers, the remaining fiber diameter is reduced to ca. 8 μm, which makes the device too fragile, especially outside of laboratory settings. For this reason, large core fibers (200–400 μm core) are privileged over standard ones. With their dimensions, they are quite easy to handle. However, they require customized connectors, splicers, and couplers. Also, increased volumes of analytes need to be used with such large fibers. These two limitations are overcome by TFBGs for instance but a constraint there remains the need for a tight control of the polarization state of the light, which is essential to ensure a proper SPR generation. So, for the moment, there is no unique solution and to reach the full potential of the technology, further developments need to be made. In order for these to materialize, a close integration of competences in various fields such as physics, photonics, biochemistry, and material science will be required.

Table 3 Detection performance of recent plasmonic optical fiber biochemical sensors

Sensor configuration	Type of excitation	Functional materials	Analyte and sensor performances	Ref.
Side-polished SMF	SPR	Au layer+SAM+antigen LP	*Legionella pneumophila* (LP) LOD 10^1 CFU (colony forming unit)/ml	[23]
Side-polished SMF	SPR	Au layer+SAM+antigen SEB	Staphylococcal enteroxin B (SEB) LOD 10 ng/ml	[24]
Unclad MMF	SPR	Ag layer+lipase enzyme	Triacylglycerides *S* 3.17 nm/mM in the range 0.5–7.0 mM	[78]
Unclad MMF	SPR	Ag, Si layers+enzyme gel	Urea *S*<0.2 nm/mM in the range 0–160 mM	[79]
Unclad MMF	SPR	Au layer+4-aminothiophenol+anti-apolipoprotein B	Low-density lipoprotein (LDL) *S* 0.18 nm/(mg/dl) in the range 0–190 mg/dl	[80]
Unclad MMF	SPR	Ag layer+tyrosinase gel	Phenolic compounds in aqueous samples LOD 38 μm for phenol to 100 μm for catechol	[81]
Unclad MMF	SPR	Au layer+nanobeads+polyclonal Ara h1 antibody	Ara h1 peanut allergens in complex food matrices LOD 0.09 μg/ml (with nanobead enhanced assay)	[82]
Unclad MMF	SPR	Au layer+SAM+streptavidin+biotinylated ssDNA aptamers	DNA hybridization assay Human immunoglobulin E (hIgE) LOD 2 nm	[83]
Unclad MMF	SPR	Au layer+ssDNA+AuNP modified ssDNA	Genetic mutations in PCR amplified DNA of bacterium *Legionella pneumophila* LOD 1 nm	[84]
Unclad MMF	SPR	Au layer+SAM+streptavidin+biotinylated eGFP (enhanced green fluorescence protein)	p3 and p8 bacteriophages binding Kinetic analysis	[85]
TFBGs	SPR	Au layer+thiol-modified aptamers	Thrombin in buffer and serum solutions LOD 22 nm	[66, 86]
TFBGs	SPR	Au layer+SAM+anti-transferrins	Transferrin LOD 10^{-6} g/ml	[87]
TFBGs	SPR	Au layer+fibronectin	Analysis of cellular behavior under different stimuli	[88]
Specialty fiber	SPR	Ag layer+SAM+biotin+neutravidin+ biotinylated anti-CLU IgG and anti-apoE IgG	Gastric cancer biomarkers: apolipoprotein E (apoE) and clusterin (CLU) Two cascaded sensing regions	[89]
End face MMF	LSPR	Spherical Au NPs+anti-IFN-γ and anti-PSA	Interferon-γ (IFN-γ) and prostate-specific antigen (PSA) LOD 2 pg/ml for IFN-γ and 1 pg/ml for PSA	[90]
End face SMF	LSPR	Au nanodisks+SAM+mouse anti-human PSA	Free prostate specific antigen (f-PSA) LOD 100 fg/ml (ca. 3 fM)	[91]
U-shaped	LSPR	Spherical Au NPs+glucose oxidase	Blood glucose Intensity changes in the range 0–250 mg/dl	[92]
Unclad MMF	LSPR	Spherical Au NPs+SAM+anti-IL-1β	Interleukin-1β (IL-1β) in synovial fluids LOD 21 pg/ml (1.2 pM)	[93]
Unclad MMF	LSPR	Au nanorods/nanospheres+human IgG	Anti-human immunoglobulin G (IgG) LOD 1.6 nm	[94]
Unclad MMF	LSPR	Spherical Au NPs+anti-TNF-α and anti-MMP-3	Tumor necrosis factor-α (TNF-α) and matrix metalloproteinases-3 (MMP-3) in synovial fluid LOD 8.2 pg/ml (0.48 pM) and 34 pg/ml (1.6 pM)	[95]
Unclad MMF	LSPR	Au nanorods+anti-CymMV and anti-ORSV	Cymbidium mosaic virus (CymMV) Odontoglossumringspot virus (ORSV) LOD 48 pg/ml for CymMV and 42 pg/ml for ORSV	[96]
Unclad POF	LSPR	Au NPs+anti SARS-CoV N proteins		[97]

Table 3 (continued)

Sensor configuration	Type of excitation	Functional materials	Analyte and sensor performances	Ref.
			Severe acute respiratory syndrome (SARS) coronavirus (CoV) nucleocapsid protein (N protein) in human serum LOD 1 pg/ml	
TFBGs	LSPR	APTMS, glutaraldehyde and cysteamine thin films+Au nanocages/nanospheres	Biotin LOD 11 pM (nanospheres) to 8 pM (nanocages)	[98]
PCF+FBG	LSPR	Oligonucleotide-functionalized Au NPs	DNA target sequences	[99]
Unclad MMF	SPR	Ag or Au layer+silicon+bromocresol purple	Ammonia LOD 10 ppm	[100]
Unclad MMF	SPR	Au layer+SiO_2+Palladium	Hydrogen LOD 0.5 %	[101]
Unclad MMF	SPR	Pd layer for H_2 Ag layer for H_2S Au+SiO_2 for moisture	H_2, H_2S, and H_2O	[102]
U-shaped	LSPR	Au NPs+4-mercaptobenzoic acid (4-MBA)+l-cysteine+cysteamine	Nitro-based explosive molecules LOD ppb for TNT vapors	[103]

Conclusion

This review of recent developments in fiber-optic-based SPR biochemical sensors shows the wide variety of approaches still being pursued around the world but also an increasing level of maturity in the field. True multidisciplinary efforts between photonics and biochemistry groups have led to impressive, environmentally and clinically relevant LODs for many substances that require detection and quantification. Another benefit of increased collaboration between photonics and biochemical groups is the development of more sophisticated experimental protocols and of more realistic error analyses. The main conclusion from all this is likely that many optical fiber SPR sensor platforms have passed the proof-of-principle level and are now ready for further development into commercial products. What is now needed is to find the proper application areas where the advantages of a fiber-based solution will warrant the investment of the significant effort required to build "whole solutions" that include the necessary hardware and software tools into systems that are user-friendly and available at a cost that is commensurate with the application. Also needed are more experiments in which sensors are tested in complex media that replicate the final application environment (blood serum and other physiological fluids, "real" mine tailing effluents, etc.). Of course, some of the more recent and exciting new developments are still very worthy of further research, in the areas of microstructured fibers and plastic optical fibers for instance, or the inclusion of graphene and other novel plasmonic materials, such as oxides and nitrides, in sensor fabrication [71, 104]. Recent publications indicate that in addition to having intrinsic tunable and adjustable plasmonic properties, combining graphene with noble metal particles and layers promises a wealth of new physics and sensing modes [105, 106]. It is hoped that this review will help in fostering further research in the field of fiber SPR sensors. This research should be carried out using the following guidelines:

- The optimization of the FOM and signal-to-noise ratio (SNR) instead of sensitivity alone, because these are the most important parameters in lowering the LOD.
- Reliability and feasibility: this is the key point for real applications. It is obvious that configurations requiring fewer fiber modifications are superior to those involving sophisticated structural changes or highly specialized fiber designs.
- Cost and process availability: most of the application areas for fiber-optic-based biochemical sensing (usually single-point devices with limited multiplexing capabilities) require low-cost solutions. Therefore, mass production (or at least easy production of multiple devices) technologies using established processes are needed. Again, this means using commercially available fibers with no structural modifications, standard coating processes in which multiple devices can be prepared simultaneously, and, in the case of grating-based devices, the use of phase or amplitude masks (instead of interferometric methods), to ensure that the devices produced are identical.

Acknowledgments This work was supported by the Belgian F.R.S.-FNRS (Associate research grant of C. Caucheteur), the European Research Council (Starting grant of C. Caucheteur – Grant agreement N° 280161), by the National Natural Science Foundation of China (Starting grant of T. Guo – Grant agreement N° 61205080), the Pearl River Scholar for Young Scientist of China (Starting grant of T. Guo – Grant agreement N° 2011J2200014), and by the Natural Sciences and Engineering Research Council of Canada.

References

1. Kreibig U, Vollmer M (1995) Optical properties of metal clusters. Springer, New York
2. Raether H (1988) Surface plasmons on smooth and rough surfaces and on gratings. Springer, Berlin
3. Maier SA (2007) Plasmonics: fundamentals and applications. Springer, New York
4. Homola J, Yee SS, Gauglitz G (1999) Surface plasmon resonance sensors: review. Sens Actuator B Chem 54:3
5. Homola J (2003) Present and future of surface plasmon resonance biosensors. Anal Bioanal Chem 377:528
6. Homola J (2006) Surface plasmon resonance based sensors. Springer, New York
7. Homola J (2008) Surface plasmon resonance sensors for detection of chemical and biological species. Chem Rev 108:462
8. Fan X, White IM, Shopova SI, Zhu H, Suter JD, Sun Y (2008) Sensitive optical biosensors for unlabeled targets: a review. Anal Chim Acta 620:8
9. Sharma AK, Jha R, Gupta BD (2007) Fiber-optic sensors based on surface plasmon resonance: a comprehensive review. IEEE Sens J 7: 1118
10. Gupta BD, Verma RK (2009) Surface plasmon resonance-based fiber optic sensors: principle, probe designs, and some applications. J Sens 1:1
11. Baldini F, Brenci M, Chiavaioli F, Giannetti A, Trono C (2012) Optical fibre gratings as tools for chemical and biochemical sensing. Anal Bioanal Chem 402:109
12. Wang XD, Wolfbeis OS (2013) Fiber-optic chemical sensors and biosensors (2008-2012). Anal Chem 85:487
13. Piliarik M, Homola J (2009) Surface plasmon resonance (SPR) sensors: approaching their limits? Opt Express 17:16505
14. Shalabney A, Abdulhalim I (2011) Sensitivity-enhancement methods for surface plasmon sensors. Laser Photonics Rev 5:571
15. Gedig E (2008) Surface chemistry in SPR technology. In: Schasfoort RBM, Tudos AJ (eds) Handbook of surface plasmon resonance. The Royal Society of Chemistry, London, Chap 6
16. Markowicz P, Law W, Baev A, Prasad P, Patskovsky S, Kabashin A (2007) Phase-sensitive time-modulated surface plasmon resonance polarimetry for wide dynamic range biosensing. Opt Express 15: 1745
17. Haes AJ, Van Duyne RP (2004) A unified view of propagating and localized surface plasmon resonance biosensors. Anal Bioanal Chem 379:920
18. Offermans P, Shaafsma MC, Rodriguez SRK, Zhang Y, Crego-Calama M, Brongersma SH, Rivas JG (2011) Universal scaling of the figure of merit of plasmonic sensors. ACS Nano 5:5151
19. Dwivedi YS, Sharma AK, Gupta BD (2008) Influence of design parameters on the performance of a surface plasmon sensor based fiber optic sensor. Plasmonics 3:79
20. Gentleman DJ, Booksh KS (2006) Determining salinity using a multimode fiber optic surface plasmon resonance dip-probe. Talanta 68:504
21. Pollet J, Delport F, Dinh Tran Thi, Wevers M, Lammertyn J (2008) Aptamer-based surface plasmon resonance probe. IEEE Sens:1187–1190. doi:10.1109/ICSENS.2008.4716654
22. Kanso M, Cuenot S, Louarn G (2008) Sensitivity of optical fiber sensor based on surface plasmon resonance: modeling and experiments. Plasmonics 3:49
23. Lin H, Tsao Y, Tsai W, Yang Y, Yan T, Sheu B (2007) Development and application of side-polished fiber immunosensor based on surface plasmon resonance for the detection of Legionella pneumophila with halogens light and 850 nm-LED. Sens Actuator A Phys 138:299
24. Slavík R, Homola J, Brynda E (2002) A miniature fiber optic surface plasmon resonance sensor for fast detection of Staphylococcal enterotoxin B. Biosens Bioelectron 17:591
25. Allsop T, Neal R, Mou C, Brown P, Rehman S, Kalli K, Webb DJ, Mapps D, Bennion I (2009) Multilayered coated infra-red surface plasmon resonance fibre sensors for aqueous chemical sensing. Opt Fiber Technol 15:477
26. Huang C, Jen C, Chao T, Wu W, Li W, Chau L (2009) A novel design of grooved fibers for fiber-optic localized plasmon resonance biosensors. Sensors 9:6456
27. Wu W, Jen C, Tsao T, Shen W, Cheng C, Chen C, Tang J, Li W, Chau L (2009) U-shaped fiber optics fabricated with a femtosecond laser and integrated into a localized plasmon resonance biosensor. Proc DTIP, Rome, Italy
28. Ahn JH, Seong TY, Kim WM, Lee TS, Kim I, Lee K (2012) Fiber-optic waveguide coupled surface plasmon resonance sensor. Opt Express 20:21729
29. Esteban Ó, Naranjo FB, Díaz-Herrera N, Valdueza-Felip S, Navarrete M, González-Cano A (2011) High-sensitive SPR sensing with indium nitride as a dielectric overlay of optical fibers. Sens Actuator B Chem 158:372
30. Navarrete M, Díaz-Herrera N, González-Cano A, Esteban Ó (2014) Surface plasmon resonance in the visible region in sensors based on tapered optical fibers. Sens Actuator B Chem 190:881
31. Chang Y, Chen Y, Kuo H, Wei P (2014) Nanofiber optic sensor based on the excitation of surface plasmon wave near fiber tip. J Biomed Opt 11:014032
32. Lin H, Huang C, Cheng G, Chen N, Chui H (2012) Tapered optical fiber sensor based on localized surface plasmon resonance. Opt Express 20:21693
33. Wieduwilt T, Kirsch K, Dellith J, Willsch R, Bartelt H (2013) Optical fiber micro-taper with circular symmetric gold coating for sensor applications based on surface plasmon resonance. Plasmonics 8:545
34. Verma RK, Sharma AK, Gupta BD (2008) Surface plasmon resonance based tapered fiber optic sensor with different taper profiles. Opt Commun 281:1486
35. Iga M, Seki A, Watanabe K (2004) Hetero-core structured fiber optic surface plasmon resonance sensor with silver film. Sens Actuator B Chem 101:368
36. Takagi K, Sasaki H, Seki A, Watanabe K (2010) Surface plasmon resonances of a curved hetero-core optical fiber sensor. Sens Actuator A Phys 161:1
37. Sai VVR, Kundu T, Mukherji S (2009) Novel U-bent fiber optic probe for localized surface plasmon resonance based biosensor. Biosens Bioelectron 24:2804
38. Nguyen H, Sidiroglou F, Collins SF, Davis TJ, Roberts A, Baxter GW (2013) A localized surface plasmon resonance-based optical fiber sensor with sub-wavelength apertures. Appl Phys Lett 103: 193116
39. Consales M, Ricciardi A, Crescitelli A, Esposito E, Cutolo A, Cusano A (2012) Lab-on-fiber technology: toward multifunctional optical nanoprobes. ACS Nano 6:3163
40. Jeong HH, Erdene N, Lee SK, Jeong DH, Park JH (2011) Fabrication of fiber-optic localized surface plasmon resonance

sensor and its application to detect antibody-antigen reaction of interferon-gamma. Opt Eng 50:124405
41. Lin Y, Zou Y, Mo Y, Guo J, Lindquist RG (2010) E-Beam patterned gold nanodot arrays on optical fiber tips for localized surface plasmon resonance biochemical sensing. Sensors 10:9397
42. Iadicicco A, Cusano A, Campopiano S, Cutolo A (2005) Thinned fiber Bragg gratings as refractive index sensors. IEEE Sens J 5:1288
43. Nemova G, Kashyap R (2006) Fiber-Bragg-grating-assisted surface plasmon-polariton sensor. Opt Lett 31:2118
44. Schuster T, Herschel R, Neumann N, Schäffer CG (2012) Miniaturized long-period fiber grating assisted surface plasmon resonance sensor. J Lightwave Technol 30:1003
45. Albert J, Shao LY, Caucheteur C (2013) Tilted fiber Bragg grating sensors. Laser Photonics Rev 7:83
46. Shevchenko Y, Albert J (2007) Plasmon resonances in gold-coated tilted fiber Bragg gratings. Opt Lett 32:211
47. Alam MZ, Albert J (2013) Selective excitation of radially and azimuthally polarized optical fiber cladding modes. J Lightwave Technol 31:3167
48. Shevchenko Y, Chen C, Dakka MA, Albert J (2010) Polarization-selective grating excitation of plasmons in cylindrical optical fibers. Opt Lett 35:637
49. Caucheteur C, Chen C, Voisin V, Berini P, Albert J (2011) A thin metal sheath lifts the EH to HE degeneracy in the cladding mode refractometric sensitivity of optical fiber sensors. Appl Phys Lett 99: 041118
50. Caucheteur C, Shevchenko Y, Shao LY, Wuilpart M, Albert J (2011) High resolution interrogation of tilted fiber grating SPR sensors from polarization properties measurement. Opt Express 19:1656
51. Caucheteur C, Voisin V, Albert J (2013) Polarized spectral combs probe optical fiber surface plasmons. Opt Express 21:3055
52. Baiad MD, Gagné M, Madore W, De Montigny E, Godbout N, Boudoux C, Kashyap R (2013) Surface plasmon resonance sensor interrogation with a double-clad fiber coupler and cladding modes excited by a tilted fiber Bragg grating. Opt Lett 38:4911
53. Bialiayeu A, Bottomley A, Prezgot D, Ianoul A, Albert J (2012) Plasmon-enhanced refractometry using silver nanowire coating on tilted fibre Bragg gratings. Nanotechnol 23:444012
54. Piliarik M, Homola J, Maníková Z, Čtyroký J (2003) Surface plasmon resonance sensor based on a single-mode polarization-maintaining optical fiber. Sens Actuator B Chem 90:236
55. Hassani A, Skorobogatiy M (2007) Design criteria for microstructured-optical-fiber-based surface-plasmon-resonance sensors. J Opt Soc Am B Opt Phys 24:1423
56. Hautakorpi M, Mattinen M, Ludvigsen H (2008) Surface-plasmon-resonance sensor based on three-hole microstructured optical fiber. Opt Express 16:8427
57. Lee HW, Schmidt M, Tyagi HK, Sempere LP, Russell PS (2008) Polarization-dependent coupling to plasmon modes on submicron gold wire in photonic crystal fiber. Appl Phys Lett 93:111102
58. Boehm J, Francois A, Ebendorff-Heidepriem H, Monro TM (2011) Chemical deposition of silver for the fabrication of surface plasmon microstructured optical fibre sensors. Plasmonics 6:133
59. Tan Z, Li X, Chen Y, Fan P (2014) Improving the sensitivity of fiber surface plasmon resonance sensor by filling liquid in a hollow core photonic crystal fiber. Plasmonics 9:167
60. Wong WC, Chan CC, Boo JL, Teo ZY, Tou ZQ, Yang HB (2013) Photonic crystal fiber surface plasmon resonance biosensor based on protein G immobilization. IEEE J Sel Top Quantum Electron 19: 4602107
61. Lu Y, Hao C, Wu B, Huang X, Wen W, Fu X, Yao J (2012) Grapefruit fiber filled with silver nanowires surface plasmon resonance sensor in aqueous environments. Sensors 12:12016
62. Gao D, Guan C, Wen Y, Zhong X, Yuan L (2014) Multi-hole fiber based surface plasmon resonance sensor operated at near-infrared wavelengths. Opt Commun 313:94
63. Cennamo N, D'Agostino G, Dona A, Dacarro G, Pallavicini P, Pesavento M, Zeni L (2013) Localized surface plasmon resonance with five-branched gold nanostars in a plastic optical fiber for biochemical sensor implementation. Sensors 13:14676
64. Cennamo N, D'Agostino G, Pesavento M, Zeni L (2014) High selectivity and sensitivity sensor based on MIP and SPR in tapered plastic optical fibers for the detection of L-nicotine. Sens Actuator B Chem 191:529
65. Lu Y, Hao C, Wu B, Musideke M, Duan L, Wen W, Yao J (2013) Surface plasmon resonance sensor based on polymer photonic crystal fibers with metal nanolayers. Sensors 13:956
66. Albert J, Lepinay S, Caucheteur C, Derosa MC (2013) High resolution grating-assisted surface plasmon resonance fiber optic aptasensor. Methods 63:239
67. Svorcik V, Siegel J, Sutta P, Mistrik J, Janicek P, Worsch P, Kolská Z (2011) Annealing of gold nanostructures sputtered on glass substrate. Appl Phys A 102:605
68. Sennett RS, Scott GD (1950) The structure of evaporated metal films and their optical properties. J Opt Soc Am A Opt Image Sci Vis 40:203
69. Cohen RW, Cody GD, Coutts MD, Abeles B (1973) Optical properties of granular silver and gold films. Phys Rev B 8:3689
70. Tu JJ, Homes CC, Strongin M (2003) Optical properties of ultrathin films: evidence for a dielectric anomaly at the insulator-to-metal transition. Phys Rev Lett 90:017402
71. Naik GV, Kim J, Boltasseva A (2011) Oxides and nitrides as alternative plasmonic materials in the optical range. Opt Express 1:1090
72. Lee H, Kim H, Park J, Jeong DH, Lee S (2010) Effects of surface density and size of gold nanoparticles in a fiber-optic localized surface plasmon resonance sensor and its application to peptide detection. Measurement Sci Technol 21:085805
73. Tou ZQ, Chan CC, Wong WC, Chen LH (2013) Fiber optic refractometer based on cladding excitation of localized surface plasmon resonance. IEEE Photonics Technol Lett 25:556
74. Lin Y, Zou Y, Lindquist RG (2011) A reflection-based localized surface plasmon resonance fiber-optic probe for biochemical sensing. Biomed Opt Express 2:478
75. Sciacca B, Monro TM (2014) Dip biosensor based on localized surface plasmon resonance at the tip of an optical fiber. Langmuir 30:946
76. Renoirt J, Debliquy M, Albert J, Ianoul A, Caucheteur C (2014) Surface plasmon resonances in oriented silver nanowire coatings on optical fibers. J Phys Chem C 118:11035
77. Ebersole RC, Miller JA, Moran JR, Ward MD (1990) Spontaneously formed functionally active avidin monolayers on metal surfaces: a strategy for immobilizing biological reagents and design of piezoelectric biosensors. J Am Chem Soc 112:3239
78. Baliyan A, Bhatia P, Gupta BD, Sharma EK, Kumari A, Gupta R (2013) Surface plasmon resonance based fiber optic sensor for the detection of triacylglycerides using gel entrapment technique. Sens Actuator B Chem 188:917
79. Bhatia P, Gupta BD (2012) Fabrication and characterization of a surface plasmon resonance based fiber optic urea sensor for biomedical applications. Sens Actuator B Chem 161:434
80. Verma R, Srivastava SK, Gupta BD (2012) Surface-plasmon-resonance-based fiber-optic sensor for the detection of low-density lipoprotein. IEEE Sens J 12:3460
81. Singh S, Mishra SK, Gupta BD (2013) SPR based fibre optic biosensor for phenolic compounds using immobilization of tyrosinase in polyacrylamide gel. Sens Actuator B Chem 186:388
82. Pollet J, Delport F, Janssen KPF, Tran DT, Wouters J, Verbiest T, Lammertyn J (2011) Fast and accurate peanut allergen detection with nanobead enhanced optical fiber SPR biosensor. Talanta 83: 1436

83. Pollet J, Delport F, Janssen KPF, Jans K, Maes G, Pfeiffer H, Wevers M, Lammertyn J (2009) Fiber optic SPR biosensing of DNA hybridization and DNA-protein interactions. Biosens Bioelectron 25:864
84. Knez K, Janssen KPF, Spasic D, Declerck P, Vanysacker L, Denis C, Tran DT, Lammertyn J (2013) Spherical nucleic acid enhanced FO-SPR DNA melting for detection of mutations in Legionella pneumophila. Anal Chem 85:1734
85. Knez K, Noppe W, Geukens N, Janssen KPF, Spasic D, Heyligen J, Vriens K, Thevissen K, Cammue BPA, Petrenko V, Ulens C, Deckmyn H, Lammertyn J (2013) Affinity comparison of p3 and p8 peptide displaying bacteriophages using surface plasmon resonance. Anal Chem 85:10075
86. Shevchenko Y, Francis TJ, Blair DAD, Walsh R, DeRosa MC, Albert J (2011) In situ biosensing with a surface plasmon resonance fiber grating aptasensor. Anal Chem 83:7027
87. Voisin V, Pilate J, Damman P, Mégret M, Caucheteur C (2014) Highly sensitive detection of molecular interactions with plasmonic optical fiber grating sensors. Biosens Bioelectron 51:249
88. Shevchenko Y, Camci-Unal G, Cuttica DF, Dokmeci MR, Albert J, Khademhosseini A (2014) Surface plasmon resonance fiber sensor for real-time and label-free monitoring of cellular behavior. Biosens Bioelectron 56:359
89. Sciacca B, François A, Hoffmann P, Monro TM (2013) Multiplexing of radiative-surface plasmon resonance for the detection of gastric cancer biomarkers in a single optical fiber. Sens Actuator B Chem 183:454
90. Jeong H, Erdene N, Park J, Jeong D, Lee H, Lee S (2013) Real-time label-free immunoassay of interferon-gamma and prostate-specific antigen using a fiber-optic localized surface plasmon resonance sensor. Biosens Bioelectron 39:346
91. Sanders M, Lin Y, Wei J, Bono T, Lindquist RG (2014) An enhanced LSPR fiber-optic nanoprobe for ultrasensitive detection of protein biomarkers. Biosens Bioelectron 61:95
92. Srivastava SK, Arora V, Sapra S, Gupta BD (2012) Localized surface plasmon resonance-based fiber optic U-shaped biosensor for the detection of blood glucose. Plasmonics 7:261
93. Chiang C, Hsieh M, Huang K, Chau L, Chang C, Lyu S (2010) Fiber-optic particle plasmon resonance sensor for detection of interleukin-1β in synovial fluids. Biosens Bioelectron 26:1036
94. Cao J, Tu MH, Sun T, Grattan KTV (2013) Wavelength-based localized surface plasmon resonance optical fiber biosensor. Sens Actuator B Chem 181:611
95. Huang Y, Chiang C, Li C, Chang T, Chiang C, Chau L, Huang K, Wu C, Wang S, Lyu S (2013) Quantification of tumor necrosis factor-α and matrix metalloproteinases-3 in synovial fluid by a fiber-optic particle plasmon resonance sensor. Analyst 138:4599
96. Lin H, Huang C, Lu S, Kuo I, Chau L (2014) Direct detection of orchid viruses using nanorod-based fiber optic particle plasmon resonance immunosensor. Biosens Bioelectron 51:371
97. Huang JC, Chang Y, Chen K, Su L, Lee C, Chen C, Chen YA, Chou C (2009) Detection of severe acute respiratory syndrome (SARS) coronavirus nucleocapsid protein in human serum using a localized surface plasmon coupled fluorescence fiber-optic biosensor. Biosens Bioelectron 25:320
98. Lepinay S, Staff A, Ianoul A, Albert J (2014) Improved detection limits of protein optical fiber biosensors coated with gold nanoparticles. Biosens Bioelectron 52:337
99. Candiani A, Bertucci A, Giannetti S, Konstantaki M, Manicardi A, Pissadakis S, Cucinotta A, Corradini R, Selleri S (2013) Label-free DNA biosensor based on peptide nucleic acid-functionalized microstructured optical fiber-Bragg grating. J Biomed Opt 18: 057004
100. Bhatia P, Gupta BD (2013) Surface plasmon resonance based fiber optic ammonia sensor utilizing Bromocresol purple. Plasmonics 8: 779
101. Perrotton C, Westerwaal RJ, Javahiraly N, Slaman M, Schreuders H, Dam B, Meyrueis P (2013) A reliable, sensitive and fast optical fiber hydrogen sensor based on surface plasmon resonance. Opt Express 21:382
102. Pfeifer KB, Thornberg SM (2010) Surface plasmon sensing of gas phase contaminants using a single-ended multiregion optical fiber. IEEE Sens J 10:1360
103. Bharadwaj R, Mukherji S (2014) Gold nanoparticle coated U-bend fibre optic probe for localized surface plasmon resonance based detection of explosive vapours. Sens Actuator B Chem 192:804
104. Wu Y, Yao B, Zhang A, Rao YJ, Wang Z, Cheng Y, Gong Y, Zhang W, Chen Y, Chiang KS (2014) Graphene-coated microfiber Bragg grating for high sensitivity gas sensing. Opt Letters 39:1235
105. Kim JA, Hwang T, Dugasani SR, Amin R, Kulkarni A, Park SH, Kim T (2013) Graphene based fiber optic surface plasmon resonance for bio-chemical sensor applications. Sens Actuator B Chem 187:426
106. Grigorenko AN, Polini M, Novoselov KS (2012) Graphene plasmonics. Nat Photonics 6:749